



# HHS Public Access

Author manuscript

*Nat Chem Biol.* Author manuscript; available in PMC 2020 August 20.

Published in final edited form as:

*Nat Chem Biol.* 2019 September ; 15(9): 925–931. doi:10.1038/s41589-019-0340-4.

## Inducible asymmetric cell division and cell differentiation in a bacterium

Nikolai V. Mushnikov<sup>1</sup>, Anastasia Fomicheva<sup>1</sup>, Mark Gomelsky<sup>1</sup>, Grant R. Bowman<sup>\*,1</sup>

<sup>1</sup>University of Wyoming Department of Molecular Biology.

### Abstract

Multicellular organisms achieve greater complexity through cell divisions that generate different cell types. We engineered a simple genetic circuit that induces asymmetric cell division and subsequent cell differentiation in *Escherichia coli*. The circuit involves a scaffolding protein, PopZ, that is stably maintained at a single cell pole over multiple asymmetric cell divisions. PopZ was functionalized to degrade the signaling molecule, c-di-GMP. By regulating synthesis of functionalized PopZ via small molecules or light, we can chemically or optogenetically control the relative abundance of two distinct cell types, characterized by either low or high c-di-GMP levels. Differences in c-di-GMP levels can be transformed into genetically programmable differences in protein complex assembly or gene expression, which in turn produce differential behavior or biosynthetic activities. This study shows emergence of complex biological phenomena from a simple genetic circuit and adds programmable bacterial cell differentiation to the genetic toolbox of synthetic biology and biotechnology.

### Graphical Abstract

---

Users may view, print, copy, and download text and data-mine the content in such documents, for the purposes of academic research, subject always to the full Conditions of use:[http://www.nature.com/authors/editorial\\_policies/license.html#terms](http://www.nature.com/authors/editorial_policies/license.html#terms)

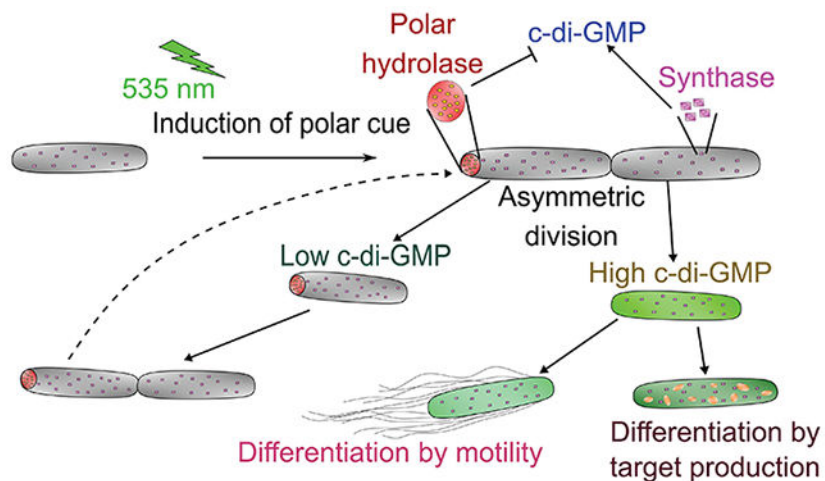
\*CONTACT INFORMATION: Grant Bowman, University of Wyoming, 1000 E. University Ave., Laramie, Wyoming 82070, Tel: 307-766-2147, [grant.bowman@uwyo.edu](mailto:grant.bowman@uwyo.edu).

#### AUTHOR CONTRIBUTIONS

NM conceived and performed experiments, collected and analyzed data, and contributed to the writing of the manuscript. AF had a similar role relating to the development of the c-di-GMP biosensor. MG guided research strategies and edited the manuscript. GB conceived experiments, guided research strategies, and wrote the manuscript.

#### COMPETING INTERESTS

No competing interests to report.



## INTRODUCTION

For multicellular organisms, the development and maintenance of tissues with multiple cell types depends on asymmetric cell divisions and subsequent cell differentiation into progeny with distinct expressional and behavioral characteristics<sup>1</sup>. For unicellular organisms such as bacteria, most depictions of cell division show daughter cells that are essentially identical in morphology and function, although a large and growing number of studies show that asymmetric cell division is also widespread in this kingdom<sup>2,3</sup>. In spore-forming bacteria, environmental conditions trigger an asymmetric cell division that generates a spore cell and a supporting mother cell<sup>4</sup>. In the Alphaproteobacterium *Caulobacter crescentus*, every cell division is asymmetric, producing a sessile and a motile daughter cell with distinct morphological, transcriptional and proteomic profiles<sup>5,6</sup>. There is also strong evidence for asymmetric cell division across *Alphaproteobacteria* and in other clades<sup>2</sup>, including *Chlamydia*<sup>7</sup>, *Myxobacteria*<sup>8</sup>, and *Mycobacteria*<sup>9</sup>.

Given the widespread occurrence of asymmetric cell division and cell differentiation across the bacterial kingdom, it is likely that the molecular mechanisms that underlie this phenomenon arose on multiple independent occasions in evolutionary history of prokaryotes<sup>10</sup>. It follows that the evolutionary process of acquiring asymmetry and cell differentiation is simpler than might be assumed from considering existing species, in which these processes are associated with a large network of genes and pathways. In *C. crescentus*, for example, the number of asymmetrically localized proteins and associated signaling factors is approximately 135<sup>11</sup>, and in spore-forming *Bacillus subtilis*, that number is 383<sup>12</sup>. Such complexity makes it difficult to discern the minimal set of components required for cell differentiation.

A goal of this study was to engineer a minimal genetic system that is sufficient for driving asymmetric cell division and cell differentiation in bacteria. Our approach was to build two interconnected subsystems in *E. coli* cells: i) a physical cue that partitions asymmetrically during cell division, and ii) a mechanism that connects the presence or absence of the physical cue to a program of gene expression.

We used the cell pole organizing protein PopZ from *Caulobacter crescentus* as a platform upon which to build an asymmetrically partitioning physical cue. PopZ's C-terminal domain drives self-assembly into oligomers and higher-order filamentous structures that combine to form a lattice-like macromolecular complex<sup>13</sup>. When PopZ is expressed in a heterologous host like *E. coli*, the self-assembling structure becomes diffusionally constrained within the bacterial nucleoid, which is the dense mixture of chromosomal DNA and associated factors that occupy most of the cell interior. Through an entropy-driven process, such large macromolecular structures are excluded from the nucleoid and therefore accumulate at the cell poles, which are nucleoid-free<sup>14,15</sup>. When PopZ is present at moderate levels in *E. coli*, PopZ structures are often found at only one of the two cell poles<sup>16,17</sup>. This is because cell division continually produces new poles at the site of the former division plane, and it is more energetically favorable to maintain an existing cluster at the old pole rather than to seed the formation of a new complex at the new pole<sup>18</sup>. Thus, when cells divide, the division is asymmetric in that the daughter cells that inherit the old pole retain a polar PopZ complex while their siblings inherit open poles.

These pole-localized PopZ complexes were used as signaling platforms to transform homogenous populations of *E. coli* cells into cultures with two differentiated cell types. To do this, we used translational fusions to link PopZ to a mechanism for controlling the level of the secondary messenger signaling molecule cyclic dimeric GMP (c-di-GMP)<sup>19,20</sup>. We chose the c-di-GMP signaling system because it can control various aspects of cellular behavior via diverse mechanisms, including changes in DNA binding activity, protein-protein interactions, and gene expression<sup>21,22</sup>. In our system, c-di-GMP signaling was linked to a transcriptional output that allowed us to differentiate cells on the basis of reporter gene expression, motility, or the activation of a synthetic multi-enzyme pathway. Our most basic circuit accomplishes asymmetric cell division and cell differentiation with only four genes. Another goal of this study was to develop technology for controlling the number and/or activities of different cell types in bioreactors, which could be beneficial to various bioengineering and biotechnology applications. To do this, we placed PopZ expression under a light-inducible promoter<sup>23,24</sup>, which allowed us to regulate the ratio of cell types through externally applied stimuli. The complete, light tunable system includes eight genes.

## RESULTS

### Design Strategy

Our general design of a genetic circuit that drives asymmetric cell division and cell differentiation included a physical cue that partitions asymmetrically during cell division and a connection from the physical cue to a signal that regulates downstream processes (Figure 1a, 1b). We used the scaffolding protein PopZ from *C. crescentus* as a platform for the asymmetrically partitioning cue. To enable phenotypic differences between daughter cells, we functionalized PopZ complexes by turning them into polar regulators of c-di-GMP concentration. To do this, we linked PopZ to a c-di-GMP degrading phosphodiesterase (PDE), YhjH (PdeH) from *E. coli*<sup>25</sup>. As the N-terminus of PopZ is structurally disordered and tolerates fusions with other proteins<sup>17</sup>, we translationally fused this end of the protein to the fluorescent protein mCherry (mChy) and YhjH.

To determine whether the tripartite YhjH-mChy-PopZ fusion retained c-di-GMP PDE activity, we expressed it in an *E. coli yhjH* mutant that is impaired in swimming through soft agar due to high c-di-GMP levels<sup>25</sup>. YhjH-mChy-PopZ rescued the swimming defect, suggesting that it retains PDE activity (Supplementary Figure 1). To determine whether YhjH-mChy-PopZ forms polar complexes that are asymmetrically distributed between dividing cells, we induced YhjH-mChy-PopZ expression for 2 h, then washed away the inducer and recorded the behavior of dividing cells by time-lapse microscopy (Figure 1c and Supplementary Video 1) and in liquid cultures (Supplementary Figure 2). YhjH-mChy-PopZ foci remained stably localized at the same cell pole for several hours, which encompassed several rounds of cell division, while daughter cells that did not inherit YhjH-mChy-PopZ foci did not produce new fluorescent foci. Therefore, the YhjH fusion did not interfere with PopZ localization, and the cells divided asymmetrically with respect to YhjH-mChy-PopZ.

To enhance the difference in intracellular c-di-GMP levels between cells that possess and lack YhjH-mChy-PopZ, we introduced a c-di-GMP synthesizing enzyme, diguanylate cyclase (DGC), to boost the background level of c-di-GMP production. DGC expression inhibited motility in our WT genetic background (Supplementary Figure 1b), indicative of increased c-di-GMP levels compared to the low baseline level<sup>26</sup>. In a combined circuit (Figure 1a, 1b), we expected that modest DGC activity could be used to raise c-di-GMP in cells lacking YhjH-mChy-PopZ, yet not be sufficient to overcome the strong c-di-GMP hydrolytic activity of YhjH-mChy-PopZ in cells containing polar YhjH-mChy-PopZ complexes.

### Split-GFP detects differential levels of c-di-GMP

To monitor c-di-GMP levels in differentiated cells, we designed a fluorescent split-protein c-di-GMP reporter. It is engineered from the *Xanthomonas campestris* proteins FimX and PilZ, whose interaction is enhanced in the presence of c-di-GMP<sup>27</sup>. We translationally fused these proteins to the components of a tri-partite split-GFP system (Supplementary Figure 3a)<sup>28,29</sup>. Beta-strand 11 (GFP<sub>11</sub>) of the GFP beta barrel was fused to the C-terminus of the c-di-GMP-binding EAL domain of FimX, and beta-strand 10 (GFP<sub>10</sub>) was fused to the N-terminus of PilZ. The remaining non-fluorescent portion of the GFP barrel, comprising beta-strands 1-9 (GFP<sub>1-9</sub>), was expressed separately. When GFP<sub>11</sub> and GFP<sub>10</sub> are in close proximity, they spontaneously form an antiparallel beta sheet that complements GFP<sub>1-9</sub> to form a fluorescent protein complex. According to our expectation, the FimX-GFP<sub>11</sub> + GFP<sub>10</sub>-PilZ + GFP<sub>1-9</sub> reporter produced fluorescence in high c-di-GMP cells expressing Slr1143, yet showed no fluorescence in the low c-di-GMP cells lacking Slr1143 (Supplementary Figure 3b).

Next, we tested c-di-GMP dependent split-GFP assembly using two genetic circuits, which differed in the level of DGC activity (Figure 2a,b). One of the variants employed the highly active DGC Slr1143<sup>23</sup>, while the other employed a less active synthetic DGC, BphS<sup>24</sup> (Supplementary Figure 1). Following a two-hour induction period, 80-90% of cells contained YhjH-mChy-PopZ and exhibited little or no GFP fluorescence. Over subsequent rounds of cell division in the absence of the inducer, the fraction of cells containing YhjH-mChy-PopZ foci decreased, while the fraction of GFP positive cells and the intensity of GFP

signal increased (Figure 2c, Supplementary Figure 4). In aliquots removed at each time point, fluorescence microscope images were consistent with flow cytometry data. Notably, the populations of YhjH-mChy-PopZ positive and GFP positive cells were distinct, as the number of double-positive cells was less than 1%. Thus, asymmetric cell division produced two cell types that could be differentiated on the basis of c-di-GMP levels. Moreover, the split-protein system also demonstrated that these cell types are functionally differentiable, on the basis of c-di-GMP dependent protein complex assembly. The flow cytometry data shows that the main cell population experiences a transient dark phase, when they have neither YhjH-mChy-PopZ nor GFP. These cells may be low in c-di-GMP because they are a small number of divisions away from an YhjH-mChy-PopZ containing ancestor, and have not yet accumulated sufficient c-di-GMP for split-GFP assembly. Consistent with this interpretation, cells expressing the stronger of the two DGCs, Slr1143, not only exhibited higher GFP levels but also had a smaller percentage of double negative cells (averaging 22%) compared to cells expressing BphS (averaging 38%).

### c-di-GMP levels drive differential gene expression

To convert asymmetric c-di-GMP distribution between daughter cells into differential gene expression patterns, we utilized a c-di-GMP-dependent transcriptional factor and reporter system from *Klebsiella pneumoniae*<sup>30</sup>. In this system, the transcriptional activator, MrkH, binds to its cognate promoter, *mrkAp*, in the presence of c-di-GMP and activates expression of the downstream gene(s)<sup>30</sup> (Figure 3a). To make the new reporter compatible with other the system components, control of *yhjH-mChy-popZ* expression was transferred to an IPTG-inducible T7 promoter.

As with our c-di-GMP-dependent split-protein reporter system (Figure 2), we observed low GFP expression levels in cells containing YhjH-mChy-PopZ and higher levels of GFP in cells lacking YhjH-mChy-PopZ (Supplementary Figures 5, 6). To accentuate this difference, we increased expression of the transcriptional activator by replacing the natural ribosome binding site (RBS) downstream of *mrkAp* with a more active RBS<sup>31</sup>. Cells containing this modified genetic circuit divided asymmetrically and differentiated into distinct YhjH-mChy-PopZ positive (GFP-negative) and GFP positive (YhjH-mChy-PopZ negative) cell populations during subsequent generations (Figure 3b, c, Supplementary Figures 7, 8 and Supplementary Videos 2, 3). Compared to the circuits that used a weaker RBS to drive *mrkH* expression, the enhanced circuit increased GFP signal in cells lacking YhjH-mChy-PopZ by six-fold (Figure 3d). As observed in strains bearing the split-GFP reporter (Figure 2), the c-di-GMP dependent signal was higher in the presence of a more active DGC, Slr1143, compared to BphS (Figure 3d and Supplementary Figures 5-8). Together, these data demonstrate that differential c-di-GMP levels in daughter cells can be readily converted to differential protein assembly or gene expression, which are the hallmarks of cell differentiation. We conclude that a circuit comprising an asymmetrically partitioning geometric cue functionalized with an enzyme for secondary messenger signaling is sufficient for establishing asymmetric cell division in bacteria.

To assess the qualities of the YhjH-mChy-PopZ control platform in our chemically inducible system, we counted the number of mChy foci per cell over time and measured their stability

(Supplementary Figure 9). After a 90 minute pulse of YhjH-mChy-PopZ expression, an average of 59% of the cells had two or more foci, often localized near opposite cell poles. As these cells divided, the percentage of YhjH-mChy-PopZ positive cells with one polar focus increased from approximately 40% to greater than 90%. In this cell type, the intensity of mChy fluorescence signal remained constant for multiple rounds of cell division (>2 hr).

Next, we asked whether our circuit can be used to control production of a bioproduct that requires a multi-enzyme biosynthetic pathway. To this end, we placed two additional coding sequences downstream of the transcriptional reporter, *gfp*: the first encoding *acyl-CoA reductase* from jojoba and the second encoding *wax ester synthase* from *Acinetobacter baylii*. The combined activity of these enzymes produces long-chain neutral lipids, like those that are naturally found in jojoba oil and spermaceti<sup>32</sup>. With this circuit, we were able to induce asymmetric cell division and generate progeny that either contained YhjH-mChy-PopZ foci or produced neutral lipids, which were detected by the lipophilic dye, BODIPY 493/503<sup>33</sup> (Figure 3e). Thus, c-di-GMP-dependent asymmetric cell division can be used to generate two distinct types of cells within an isogenic culture, which can be programmed to run different biosynthetic programs.

### Optogenetic control

Small-molecule inducers are often impractical for temporal control of gene induction because they cannot be readily removed from liquid cultures, especially those growing in large vessels. We therefore sought to replace the chemically controlled circuits in our genetic system with optogenetic circuits, where external light would control cell behavior. To accomplish this, we incorporated several components of a photo-controllable transcriptional regulation system<sup>34</sup> (Figure 4a). These included a light-activated histidine kinase, CcaS, and two additional genes needed for synthesizing its phycocyanobilin chromophore, the cognate response regulator, CcaR, and the CcaR-dependent promoter, *ccaRp*. When stimulated by green light, CcaS phosphorylates and activates CcaR, which upregulates expression from the *ccaRp* promoter. Red light irradiation inactivates CcaS kinase activity<sup>23</sup>.

We placed the *yhjH-mChy-popZ* module under control of the *ccaRp* promoter, thus bringing expression of the asymmetrically positioning cue under light control. To test for optogenetic control of asymmetric cell division and programmable gene expression, we exposed cells to intermittent pulses of green (535 nm) light for three hours, which was sufficient to induce the formation of polar YhjH-mChy-PopZ foci in >80% of cells, then initiated asymmetric cell division by switching the cultures to constant red (650 nm) light (Figure 4b,c). After four hours of incubation in red light, the fraction of YhjH-mChy-PopZ positive cells was reduced to < 10%, indicating that the cells divided and produced progeny lacking YhjH-mChy-PopZ. Next, we exposed the culture to two additional cycles of pulsed green / constant red light, while maintaining growth in log phase (Figure 4c). We observed that the population of YhjH-mChy-PopZ positive cells was restored during the period of green light exposure, and returned to 10% during subsequent exposure to constant red light. This shows that light can be used to modulate the ratio of cell types in the population for prolonged periods of time and over repeated light exposure cycles. When MrkH was induced in this system, cells lacking YhjH-mChy-PopZ expressed the GFP reporter (Supplementary Figure

10a). Together, these results demonstrate the utility of an optogenetic circuit for establishing two distinct cell types in *E. coli* culture and controlling the relative population frequencies of those cell types.

We were able to maintain stable populations of YhjH-mChy-PopZ positive cells under pulsed red / green light and PopZ negative cells under continuous red light. The growth rates of these cultures provided an indication of the doubling time of these two distinct cell types (Supplementary Figure 10b, c). YhjH-mChy-PopZ positive cells divided more slowly, with a doubling time of 35 minutes compared to 29 minutes for PopZ negative cells. This is qualitatively and quantitatively consistent with previous reports, in which newborn cells that inherited the old pole, where YhjH-mChy foci are stably maintained (Supplementary Video 1), divided more slowly than their siblings, and the presence of aggregated protein foci at old cell poles exacerbated this difference<sup>35,36</sup>.

To demonstrate that the optogenetic circuit can be used to differentiate cells on the basis of a physical trait, we chose to regulate cell motility. To this end, we placed the *motA-motB* coding sequence downstream of the *gfp* reporter, which allowed us to control the production of the MotA-MotB stators that power flagellar motors. We introduced this variant of our genetic circuit into a non-motile *motA-motB* strain background. Continuous exposure to red light activated output gene expression from the *mrkA* promoter and rescued the motility defect in soft agar (Figure 4d). Although high levels of c-di-GMP normally inhibit motility, high levels of MotA-MotB expression can overcome this effect<sup>37</sup>. To show that non-motile YhjH-mChy-PopZ cells can be induced to divide asymmetrically and produce motile progeny, we compared a culture grown in pulsed green light to one that had been switched to continuous red light, by observing cells under a fluorescence microscope (Figure 4e) and tracking their motility in liquid suspension (Figure 4f, g and Supplementary Videos 3-8). Nearly all of the cells exposed to pulsed green light contained YhjH-mChy-PopZ foci, and these cells were non-motile, as predicted by their behavior in soft agar (Figure 4d). By contrast, the culture that was induced to divide asymmetrically by switching to continuous red light consisted mostly of cells that did not carry YhjH-mChy-PopZ foci and instead expressed GFP. In this mixed population, most cells were highly motile, though the small fraction of cells that had retained YhjH-mChy-PopZ foci remained non-motile. This experiment demonstrates an optogenetic circuit that controls cell motility and gene expression through light-regulated patterning of asymmetric cell division and cell differentiation.

## DISCUSSION

For multicellular life forms, asymmetric cell division and differentiation are fundamental to the generation of tissues, organs and related aspects of organismal complexity. In this work, we created synthetic genetic circuits that drive a program of asymmetric cell division and cell differentiation in *E. coli* cells. Given that *E. coli* cells normally divide into progeny that are not easily distinguishable in morphology or behavior, we suggest that these engineered functionalities, despite the simplicity of the underlying circuitry, significantly increase the biological sophistication of the organism.

The basic version of our circuit involves only four genes: the asymmetrically localized phosphodiesterase platform, a diguanylate cyclase, a c-diGMP dependent transcription factor, and its cognate promoter. This system works because it operates within the context of other mechanisms that already exist in normal *E. coli*, particularly those responsible for targeting aggregates to cell poles<sup>14,38</sup>. A key difference is that natural *E. coli* use the sequestration of polar aggregates as a way of limiting damage to the cytoplasm<sup>36</sup>, whereas our synthetic genetic circuit uses this sequestration mechanism to position the YhjH-mChy-PopZ signaling platform for driving cell differentiation. Thus, a large leap in biological sophistication emerges from the introduction of a small set of genes whose activities build new functionalities on top of endogenous mechanisms.

While our simple synthetic circuits do not control as many traits as are observed in differentiated cells of natural asymmetrically dividing bacteria, and the process of differentiation is slower in our system than in *C. crescentus* and other species, we suggest that they provide a basic form of cell differentiation from which a more complex system could subsequently evolve. As macromolecular structures that direct cell fate and are asymmetrically inherited through multiple cell divisions, the YhjH-mChy-PopZ “control platforms” of this study bear similarity to the endogenous polar organizing proteins found in *Alphaproteobacteria*<sup>3,17</sup>, *Gammaproteobacteria*<sup>39</sup>, and also germ granules found in *Drosophila* and other eukaryotic organisms<sup>40</sup>. Evidence suggests that germ granule nucleation proteins evolved convergently in disparate eukaryotic lineages<sup>41</sup>. Thus, it may be that stable macromolecular assemblies have provided a starting point for asymmetric inheritance and cell differentiation at multiple points in prokaryotic and eukaryotic evolutionary history.

This work provides a novel set of genetic components to the expanding synthetic biology toolbox. Compared with other tools available to synthetic biologists, their novelty lies in the use of self-assembling macromolecular complexes as asymmetrically positioning cues to program cell behavior. Notably, the underlying biological mechanisms exist in natural systems. PopZ is used as a polar cue in the asymmetrically dividing bacterium *C. crescentus*<sup>42</sup>, and asymmetric distribution of c-di-GMP has been implicated in driving differential cell fate in *C. crescentus*<sup>43</sup> and other bacteria<sup>44</sup>. c-di-GMP itself is not unique as a bacterial signaling molecule, and might be replaced with other nucleotide or non-nucleotide second messengers in modified versions of our genetic circuits. Further, the flexible N-terminus of PopZ could be fused to a wide variety of functional outputs, including kinases<sup>45</sup>, adaptors for targeted proteolysis<sup>43</sup>, or components borrowed from non-bacterial organisms. To generate complex bacterial communities with more than two programmable cell types, it may be possible to employ orthogonal regulatory mechanisms as sub-routines of the existing genetic circuit.

The ability to induce asymmetric cell division in a bacterial culture and activate different genetic programs in each cell type may open the door to new biotechnological applications. For example, it may be possible to reduce the fitness cost of expressing multiple enzymes in a complex biosynthetic pathway by expressing different parts of the pathway in different cell types<sup>46</sup>. Further, the cell types’ metabolic states may be differentially tuned to optimize the activity of specific enzymes<sup>47</sup>. Analogous strategies have been used to increase production

in multi-strain co-culture systems<sup>48</sup>. When the biosynthetic pathway includes enzymes or products that are highly toxic, it may be beneficial to maintain a sub-population of regenerative, non-producing cells that are shielded from stress and can be used to generate new producer cells. Cell differentiation might also provide a means for physical separation of cell types, based on adhesion<sup>49</sup> or flocculation<sup>50</sup>. This may be useful for harvesting product from a specific cell type or maintaining it in a specialized environment.

## ONLINE METHODS

### Bacterial Strains and Plasmids

DH5 $\alpha$ : recombination deficient strain of *E.coli* used for cloning procedures.

MG-1655: K-12 wildtype strain used for some experiments, including positive control for swarmer motility tests.

MG-1655 *yjhH*<sup>1,2</sup>: mutant version of MG-1655 with high c-di-GMP level. Used as a negative control for swarmer motility tests.

MG-1655 DE3 (this work): MG-1655 derivative capable of gene expression using pT7 regulation system (was used for experiments with asymmetric cell division induction).

MG-1655 DE3 *motA-motB* (this work): non-motile derivative of MG-1655 DE3. Was made using Lambda Red recombination<sup>3</sup>, where *kanR* gene replaced part of *motA-motB* coding sequence.

### DNA Cloning

Plasmid's names and their major features are summarized in Supplementary Table S1.

The *yjhH-mChy-popZ* coding sequence was initially cloned into pBAD vector via Isothermal Gibson assembly, resulting in the pBAD-YmP plasmid. The template sequence of *mChy-popZ* was taken from the Bowman lab collection (previously unpublished). The coding sequence of *yjhH* was previously published<sup>4</sup>, as was the pBAD-YmP plasmid backbone<sup>4</sup> that was used for further insertions of *tet-p-bphS* or *et-p-slr* constructs, resulting in pBAD-YmP-B and pBAD-YmP-S plasmids, accordingly. For subsequent constructs, the whole coding sequence region was amplified and transferred into a pACYC-duet plasmid, from which the expression of YjhH-mChy-PopZ was controlled by the T7 promoter system, resulting in pAC-YmP-B and pAC-YmP-S plasmids.

To design the tripartite split-GFP reporter system, we used the FimX-c-di-GMP-PilZ structure<sup>5</sup> (PDB # 4F48) to model the positions of the GFP<sub>10</sub> and GFP<sub>11</sub> beta-strands if placed at the N- or C-termini of FimX' (EAL domain of FimX (437-684 aa)) and PilZ, with the goal of predicting an arrangement that will (i) position GFP<sub>10</sub> and GFP<sub>11</sub> in the proximity of each other and (ii) create no sterical interference between the FimX-c-di-GMP-PilZ complex and reconstructed GFP. We chose to fuse GFP<sub>10</sub> to the N-terminus of PilZ and GFP<sub>11</sub> to the C-terminus of FimX'. GFP<sub>10</sub> and GFP<sub>11</sub> were fused to PilZ and FimX', respectively, via 10-aa long flexible GS-linkers. To clone the DNA constructs, nucleotide sequences encoding FimX' (*XccFimX*<sup>EAL</sup>, residues 437-684 aa), PilZ (*XccPilZ*<sub>1028</sub>), and

split GFP fragments (GFP<sub>10</sub>, GFP<sub>11</sub> and GFP<sub>1-9</sub>) were codon-optimized and synthesized *in vitro* (Eurofins Genomics). The final construct was inserted via Gibson assembly into plasmid pMQ132.

The coding sequence for transcription factor MrkH, followed by bi-directional terminator was amplified from the template plasmid used in a previous study<sup>4</sup>, was cloned into the pBAD vector via isothermal Gibson assembly, resulting in the pBAD-MrkH plasmid. Subsequently, the *mrkAp* promoter sequence from the same study<sup>4</sup>, together with *gfp* coding sequence were cloned downstream of the terminator, in the opposite transcriptional direction to *mrkH*, resulting in a pB-Mrk-GFP plasmid. As an alternative, *MrkAp-gfp* was modified by insertion of a stronger RBS upstream GFP. Isothermal assembly of *mrkAp-rbs* and *gfp* into pBAD-MrkH vector produced the plasmid pB-Mrk-rbsGFP.

The coding sequences of enzymes used for neutral lipid biosynthesis were first cloned as a poly-cistronic message under *araBADp*-promoter. The gene encoding *acetyl-CoA reductase* from Jojoba plant was codon-optimized for expression in *E.coli* and chemically synthesized (IDT). *WE-synthase* gene was PCR-amplified from the *Acinetobacter baylii* (A kind Gift of Phoebe Lostroh, Colorado College). These were cloned into pBAD-vector by Gibson assembly, then amplified (including an RBS from *araBADp* promoter) and cloned downstream of GFP in pCDF:pMrkA-GFP(-) plasmid, made previously (a backbone vector with for insertion genes of interest downstream of GFP in a designed restriction sites, under the control of *mrkAp* promoter). Finally, the whole message including *mrkAp-gfp-ac-CoA reductase-WE-synthase* was amplified and cloned into a pBAD-MrkH vector, in the same manner as previously described for *mrkAp-gfp* message. The resulting plasmid pBAD-M-G-W is a c-di-GMP dependent system for a control of expression of GFP and waxy ethers biosynthesis pathway.

To make a system for light-regulated control of PopZ expression, we used plasmids pSR58-6 and pNO286-3, containing components for light-dependent expression of genes<sup>6</sup>, kindly given us by Jeff Tabor of Rice University, as a backbone for further cloning. Insertion of *yhjH-mCherry-popZ* under the *PcpcG2-172* promoter (later called *ccaRp*) was made via Isothermal Gibson assembly: pSR58-6 plasmid was PCR linearized (excluding *gfp* gene), and PCR-amplified *yhjH-mCherry-popZ* coding sequence was inserted in place of GFP, resulting in pCRP plasmid. The whole message encoding *araBAD-p-mrkH-mrkAp-GFP* was amplified from pB-Mrk-rbsGFP plasmid and inserted into PCR-linearized pCRP plasmid, between *CamR* and *CcaR* genes, resulting in pCRPMG plasmid. The message encoding *tet-p-slr* expression module was introduced into pNO286-3 plasmid, between *pcyA* and *specR* genes, via Isothermal Gibson assembly where insertion and vector were PCR amplified, resulting in pCSTS plasmid.

To create strain, MG-1655 DE3 *motA-motB*, Lambda Red recombination<sup>3</sup> was used to replace part of the *motA-motB* coding sequence with *kanR* coding sequence from plasmid pET28a (Novagen). The sequences of *motA-motB* bordering the *kanR* gene are GTTAACGCCTGACGACTGAACATCCTGTTCATGGTCAACAGTGGGAAGGATGATGTC and CCGTGGCTTTTGGCTTTGCGTCGTTTGACGACAATAATCGGATGCGCTTGATTCT

## Experimental procedure for induction of asymmetric cell division in *E.coli*

Cells were grown at 37°C overnight in LB media, with the addition of appropriate antibiotics. Subsequently, cultures were diluted 100 times and grown on a rotary drum in 2 ml volume in glass tubes for 2 hours prior to protein expression activation. Induction of YhjH-mChy-PopZ fusion protein was performed using 0.2% of Arabinose for two hours (in case of pBAD transcription control), or 1.5 hours using 0.02mM IPTG (in case of pT7 mediated transcription control). Inducer was removed by three repeats of pelleting cells with a micro-centrifuge at 9000 rpm and resuspending in fresh media. Prior to the subsequent chase period, cells were diluted 5 times and incubated at 37°C in 150ml flasks with shaking at 250rpm. Growing bacterial cultures were continuously diluted by removing part of media with growing cells and adding fresh media to keep the culture in a log growth phase, with OD(600) in a range between 0.3 to 0.6. For induction of MrkH expression from the pBAD promoter, 0.2% of arabinose was added to the media.

## Light Control

Cells carrying pCRPMG and pCSTS plasmids were grown overnight at 37C under illumination with 650 nm red light. Overnight cultures were diluted 100 times and grown in 2 ml volume in glass tubes with vigorous shaking under alternating illumination with 650 nm Red light (45 min) and 535 nm Green light (15min) for three hours, to ensure induction of PopZ expression. Cultures were then diluted twenty times and released in 4 ml volume in culture tubes and incubated (with shaking) under red light for 2 hours, and subsequently diluted ten-fold to maintain growth in early log phase during the next two hours of red light illumination. To re-induce PopZ expression, the cultures were diluted twenty-fold and incubated for an additional three hours (with shaking) under alternating Red/Green light illumination, as described above. The complete cycle of YhjH-mChy-PopZ induction and chase was repeated three times with periodic dilution, as described above, to maintain log phase growth. Appropriate antibiotics were used in the growth media for all stages. The whole experiment was performed twice, and these results are shown in Figure 4c.

To express MrkH, and, accordingly, circuit output (GFP/MotA-MotB proteins), 0.2% L-arabinose was added during the chase period.

The synthetic DGC BphS that was used for some experiments includes a phytochrome domain that can be activated by 650nm light<sup>4</sup>. In this work, cells expressing BphS were incubated in the dark or under ambient room lighting and at 37°C (light activation does not enhance BphS activity at this temperature). We did not explore the effects of BphS light activation mechanism in this work.

## Fluorescence Microscopy

Cells were immobilized on a 1% agarose pads. Live-cell imaging was performed using a Zeiss Axio Imager Z2 epifluorescence microscope equipped with a Hamamatsu Orca-Flash4.0 sCMOS camera and a Plan-Apochromat 100x/1.46 Oil Ph3 objective. Zeiss Filter sets 38HE and 63HE were used to acquire fluorescent images of msfGFP and mCherry, respectively. Images were collected and processed with Zen Blue software. For image panels, fluorescent signal from the YhjH-mChy-PopZ fusion (red) and GFP (green), or the

YhjH-mChy-PopZ fusion (red) and BODIPY signal (yellow) are overlaid on a phase contrast image (grayscale). Every fluorescence microscopy experiment was repeated multiple times (as indicated in the figure legend) under the conditions described, which provided similar results. The figures show data from a single trial.

### Quantification of fluorescent microscopy data

Analysis of fraction of cells with and without PopZ foci, as well as cells with different number of PopZ foci at different stages of experiments (Figure S6, Figure S7) was done using Cell Counter plugin for ImageJ software. The quantification process was not formally blinded, but at the time of scoring the image files had names that obscured their relevance to the experiment.

### Measuring of the growth rate of bacterial cultures

For quantification of the growth rate (Figure S7 a), exponentially growing culture was sampled hourly and OD600 was measured. The experimental measurements were scattered in logarithmic format in MS Excel and linear fragment of the resulted curves were used for doubling time calculations, using:  $r = (\ln [OD2/OD1]) / (T2-T1)$ . Doubling time corresponds to  $\ln 2/r$ .

### Time-lapse microscopy

For time-lapse microscopy experiments, cells were immobilized on the 1.2% low-temperature melting agarose (ultra PURE LMP agarose, GIBCO BRL, Life Technologies Inc.) pads. Fluorescent images were taken with the same settings as described above, with image capture at 20 min intervals.

### Flow Cytometry

Samples of cells (200 $\mu$ l) were fixed in 4%PFA for 30 min, then washed and incubated in PBS, and stored at 4°C until future analysis. 100,000 to 500,000 cells from each sample were analyzed by flow cytometry using a Yeti cell analyzer (Propel Labs, Ft. Collins, CO; now known as ZE5, BioRad, Hercules, CA) using Everest software. Cells were gated using linear forward scatter (FS) by log side scatter (SS), followed by gating on FS area by FS height for aggregate exclusion. Fluorescence was collected using a 525/35 nm filter from the 488 nm laser line for GFP and a 615/20 nm filter from the 561 nm laser line for mCherry. Kaluza analysis software (Beckman Coulter Life Sciences, Indianapolis, IN) was used for data analysis. Analysis occurred under blinded conditions. On all plots of flow cytometry data, fluorescence intensity in GFP and mChy channels is plotted on the X and Y axis, respectively. Where strains are directly compared (e.g. Figure 3d), strains were grown simultaneously and under the same conditions. Each experiment was repeated in six separate trials that produced similar results. All samples were collected, prepared, stored, and analyzed by the same methods. The plots show data from a single trial, and the distribution of events is represented by a colored density plot.

### Staining of neutral lipids

Samples were fixed in 4% PFA (30 min), then washed in PBS and stained with BODIPY (488nm) for 10 min, according to manufacturer instructions.

### Motility Assays

To test motility on plates, 3µl of log-phase cells were spotted onto semi-solid agar (1% Tryptone, 0.5% Sodium Chloride, 0.25% Agar), and grown 7 hours at 37°C under green (525nm) or red light (650nm). To observe cell motility by microscopy, 10 µl of cell culture was mounted on a glass slide by placing the drop between two #1.5 coverslips, then covering it with a third #1.5 coverslip. Videos of motile and non-motile cells were recorded using the streaming mode of a Hamamatsu Orca-Flash4.0 sCMOS camera mounted on a Zeiss Axio Imager Z2 epifluorescence microscope, viewed through a Plan-Apochromat, 20x/0.18 Oil Ph1 objective. Phase contrast and fluorescence movies (filter 63HE) consisted of 500 image frames, acquired continuously with 30ms exposure times, and were acquired independently but in rapid succession, focused on the same field. The TrackMate plugin for ImageJ was used to analyze these movies in order to track cell motility.

### DATA AVAILABILITY STATEMENT

The datasets generated during and/or analyzed during the current study are available from the corresponding author on request.

### Supplementary Material

Refer to Web version on PubMed Central for supplementary material.

### ACKNOWLEDGEMENTS

The authors would like to thank Jeff Tabor for providing plasmids related to the light inducible transcription activation system. Naomi Ward provided reagents and equipment. Karen Helm and Christine Childs, from the Flow Cytometry Shared Resource at the University of Colorado Cancer Center, were supported by the Cancer Center Support Grant P30CA046934. This work was supported by School of Energy Resources at the University of Wyoming and by the National Institutes of Health under award numbers 2P20GM103432 and R01GM118792.

### REFERENCES

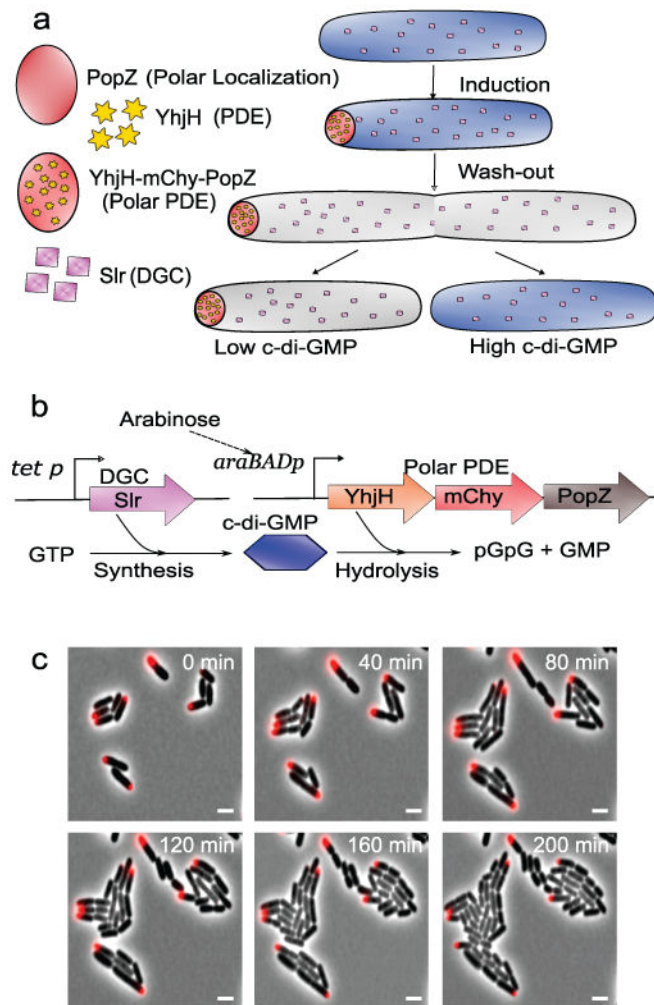
1. Inaba M & Yamashita YM Asymmetric stem cell division: Precision for robustness. *Cell Stem Cell* 11, 461–469 (2012). [PubMed: 23040475]
2. David T Kysela<sup>1</sup>, Pamela J.B. Brown<sup>2</sup>, Kerwyn Casey Huang<sup>3, 4</sup>, and Y. V. B. Biological Consequences and Advantages of Asymmetric Bacterial Growth. *Annu Rev Microbiol*, 67, 417–435 (2013). [PubMed: 23808335]
3. Ehrle HM et al. Polar organizing protein PopZ is required for chromosome segregation in *Agrobacterium tumefaciens*. *J. Bacteriol.* 199, (2017).
4. Tan IS & Ramamurthi KS Spore formation in *Bacillus subtilis*. *Environ. Microbiol. Rep.* 6, 212–225 (2014). [PubMed: 24983526]
5. Tsokos CG & Laub MT Polarity and cell fate asymmetry in *Caulobacter crescentus*. *Curr. Opin. Microbiol.* 15, 744–750 (2012). [PubMed: 23146566]
6. Grünenfelder B et al. Proteomic analysis of the bacterial cell cycle. *Proc. Natl. Acad. Sci. U. S. A.* 98, 4681–4686 (2001). [PubMed: 11287652]

7. Abdelrahman Y, Ouellette SP, Belland RJ & Cox JV Polarized Cell Division of *Chlamydia trachomatis*. *PLoS Pathog.* 12, 1–20 (2016).
8. Sogaard-Andersen DS and Regulation of motility L and polarity in *Myxococcus xanthus*. *Annu. Rev. Microbiol.* 71, 61–78 (2017). [PubMed: 28525300]
9. Logsdon MM & Aldridge BB Stable regulation of cell cycle events in mycobacteria: Insights from inherently heterogeneous bacterial populations. *Front. Microbiol* 9, 1–15 (2018). [PubMed: 29403456]
10. Lyons NA & Kolter R On the evolution of bacterial multicellularity. *Curr. Opin. Microbiol* 24, 21–28 (2015). [PubMed: 25597443]
11. Werner JN et al. Quantitative genome-scale analysis of protein localization in an asymmetric bacterium. *Proc. Natl. Acad. Sci* 106, 7858–7863 (2009). [PubMed: 19416866]
12. Eichenberger P et al. The program of gene transcription for a single differentiating cell type during sporulation in *Bacillus subtilis*. *PLoS Biol.* 2, 1664–1683 (2004).
13. Bowman GR et al. Oligomerization and higher-order assembly contribute to sub-cellular localization of a bacterial scaffold. *Mol. Microbiol* 90, 776–95 (2013). [PubMed: 24102805]
14. Coquel AS et al. Localization of Protein Aggregation in *Escherichia coli* Is Governed by Diffusion and Nucleoid Macromolecular Crowding Effect. *PLoS Comput. Biol* 9, 1–14 (2013).
15. Neeli-Venkata R et al. Robustness of the process of nucleoid exclusion of protein aggregates in *Escherichia coli*. *J. Bacteriol* 198, 898–906 (2016). [PubMed: 26728194]
16. Ebersbach G, Briegel A, Jensen GJ & Jacobs-Wagner C A Self-Associating Protein Critical for Chromosome Attachment, Division, and Polar Organization in *Caulobacter*. *Cell* 134, 956–968 (2008). [PubMed: 18805089]
17. Holmes JA et al. *Caulobacter* PopZ forms an intrinsically disordered hub in organizing bacterial cell poles. *Proc. Natl. Acad. Sci* 113, 12490–12495 (2016). [PubMed: 27791060]
18. Scheu K, Gill R, Saberi S, Meyer P & Emberly E Localization of aggregating proteins in bacteria depends on the rate of addition. *Front. Microbiol* 5, 1–5 (2014). [PubMed: 24478763]
19. Simm R, Morr M, Kader A, Nimtz M & Römling U GGDEF and EAL domains inversely regulate cyclic di-GMP levels and transition from sessility to motility. *Mol. Microbiol* 53, 1123–1134 (2004). [PubMed: 15306016]
20. Ryu M & Gomelsky M Near-infrared Light Responsive Synthetic c – di-GMP Module for Optogenetic Applications. *ACS Synth. Biol.* 11, 802–810 (2013).
21. Jenal U, Reinders A & Lori C Cyclic di-GMP: Second messenger extraordinaire. *Nat. Rev. Microbiol.* 15, 271–284 (2017). [PubMed: 28163311]
22. Chou SH & Galperin MY Diversity of cyclic di-GMP-binding proteins and mechanisms. *J. Bacteriol* 198, 32–46 (2016). [PubMed: 26055114]
23. Schmidl SR, Sheth RU, Wu A & Tabor JJ Refactoring and optimization of light-switchable *Escherichia coli* two-component systems. *ACS Synth. Biol* 3, 820–831 (2014). [PubMed: 25250630]
24. Tabor JJ, Levskaya A & Voigt C a. Multichromatic control of gene expression in *Escherichia coli*. *J. Mol. Biol* 405, 315–324 (2011). [PubMed: 21035461]
25. Ryjenkov D. a, Simm R, Römling U & Gomelsky M The PilZ domain is a receptor for the second messenger c-di-GMP: the PilZ domain protein YcgR controls motility in Enterobacteria. *J. Biol. Chem* 281, 30310–4 (2006). [PubMed: 16920715]
26. Boehm A et al. Second Messenger-Mediated Adjustment of Bacterial Swimming Velocity. *Cell* 141, 107–116 (2010). [PubMed: 20303158]
27. Chin KH et al. Structural polymorphism of c-di-GMP bound to an EAL domain and in complex with a type II PilZ-domain protein. *Acta Crystallogr. Sect. D Biol. Crystallogr* 68, 1380–1392 (2012). [PubMed: 22993092]
28. Cabantous S et al. A new protein-protein interaction sensor based on tripartite split-GFP association. *Sci. Rep* 3, 2854 (2013). [PubMed: 24092409]
29. Shekhawat SS & Ghosh I Split-protein systems: Beyond binary protein-protein interactions. *Curr. Opin. Chem. Biol* 15, 790–797 (2011).

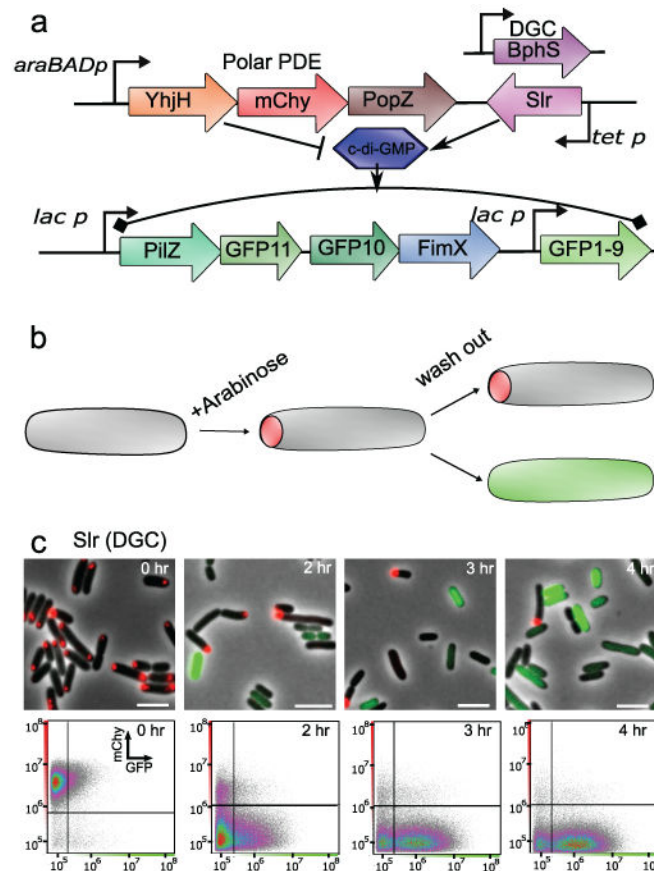
30. Wilksch JJ et al. MrKH, a novel c-di-GMP-dependent transcriptional activator, controls *Klebsiella pneumoniae* biofilm formation by regulating type 3 fimbriae expression. *PLoS Pathog.* 7, (2011).
31. Guzman L-M, Belin D, Carson MJ & Beckwith J Tight Regulation, Modulation, and High-Level Expression by Vectors Containing the Arabinose P BAD Promoter. *J. Bacteriol* 177, 4121–4130 (1995). [PubMed: 7608087]
32. Kalscheuer R et al. Neutral Lipid Biosynthesis in Engineered *Escherichia coli*: Jojoba Oil-Like Wax Esters and Fatty Acid Butyl Esters. *Appl. Environ. Microbiol* 72, 1373–1379 (2006). [PubMed: 16461689]
33. Harris LALS, Skinner JR & Wolins NE Imaging of Neutral Lipids and Neutral Lipid Associated Proteins. *Methods Cell Biol.* 116, 213–226 (2013). [PubMed: 24099295]
34. Ong NTX & Tabor JJ A miniaturized *E. coli* green light sensor with high dynamic range. *ChemBioChem*, 19, 1255–1258 (2018). [PubMed: 29420866]
35. Lindner a. B., Madden R, Demarez a., Stewart EJ & Taddei F Asymmetric segregation of protein aggregates is associated with cellular aging and rejuvenation. *Proc. Natl. Acad. Sci* 105, 3076–3081 (2008). [PubMed: 18287048]
36. Winkler J et al. Quantitative and spatio-temporal features of protein aggregation in *Escherichia coli* and consequences on protein quality control and cellular ageing. *EMBO J.* 29, 910–923 (2010). [PubMed: 20094032]
37. Paul K, Nieto V, Carlquist WC, Blair DF & Harshey RM The c-di-GMP Binding Protein YcgR Controls Flagellar Motor Direction and Speed to Affect Chemotaxis by a ‘Backstop Brake’ Mechanism. *Mol. Cell* 38, 128–139 (2010). [PubMed: 20346719]
38. Lloyd-Price J et al. Asymmetric disposal of individual protein aggregates in *Escherichia coli*, one aggregate at a time. *J. Bacteriol* 194, 1747–1752 (2012). [PubMed: 22287517]
39. Rossmann FM et al. The GGDEF domain of the phosphodiesterase PdeB in *Shewanella putrefaciens* mediates recruitment by the polar landmark protein HubP. *J. Bacteriol* 49, (2019).
40. Smith J et al. Spatial patterning of P granules by RNA-induced phase separation of the intrinsically-disordered protein MEG-3. *Elife* 5, 1–18 (2016).
41. Kulkarni A & Extavour CG Convergent evolution of germ granule nucleators: A hypothesis. *Stem Cell Res.* 24, 188–194 (2017). [PubMed: 28801028]
42. Bergé M & Viollier PH End-in-Sight: Cell Polarization by the Polygamic Organizer PopZ. *Trends Microbiol.* 26, 363–375 (2018). [PubMed: 29198650]
43. Lori C, Ozaki S, Steiner S, Bohm R, Abel S, Dubey BN, Schirmer T, S. H. & U. J. Cyclic di-GMP acts as a cell cycle oscillator to drive chromosome replication. *Nature* 523, (2015).
44. Christen M et al. Asymmetrical distribution of the second messenger c-di-GMP upon bacterial cell division. *Science* 328, 1295–1297 (2010). [PubMed: 20522779]
45. Zschiedrich CP, Keidel V & Szurmant H Molecular Mechanisms of Two-Component Signal Transduction. *J. Mol. Biol* 428, 3752–3775 (2016). [PubMed: 27519796]
46. Tsoi R et al. Metabolic division of labor in microbial systems. *Proc. Natl. Acad. Sci. U. S. A* 115, 2526–2531(2018). [PubMed: 29463749]
47. Doong SJ, Gupta A & Prather KLJ Layered dynamic regulation for improving metabolic pathway productivity in *Escherichia coli*. *Proc. Natl. Acad. Sci* 115, 2964–2969 (2018). [PubMed: 29507236]
48. Zhang H & Stephanopoulos G Co-culture engineering for microbial biosynthesis of 3-amino-benzoic acid in *Escherichia coli*. *Biotechnol. J* 11, 981–987 (2016). [PubMed: 27168529]
49. Jin X & Riedel-Kruse IH Biofilm Lithography enables high-resolution cell patterning via optogenetic adhesin expression. *Proc. Natl. Acad. Sci* 115, 3698–3703 (2018). [PubMed: 29555779]
50. Ojima Y, Nguyen MH, Yajima R & Taya M Flocculation of *Escherichia coli* cells in association with enhanced production of outer membrane vesicles. *Appl. Environ. Microbiol* 81, 5900–5906 (2015). [PubMed: 26092467]

## ONLINE METHODS REFERENCES

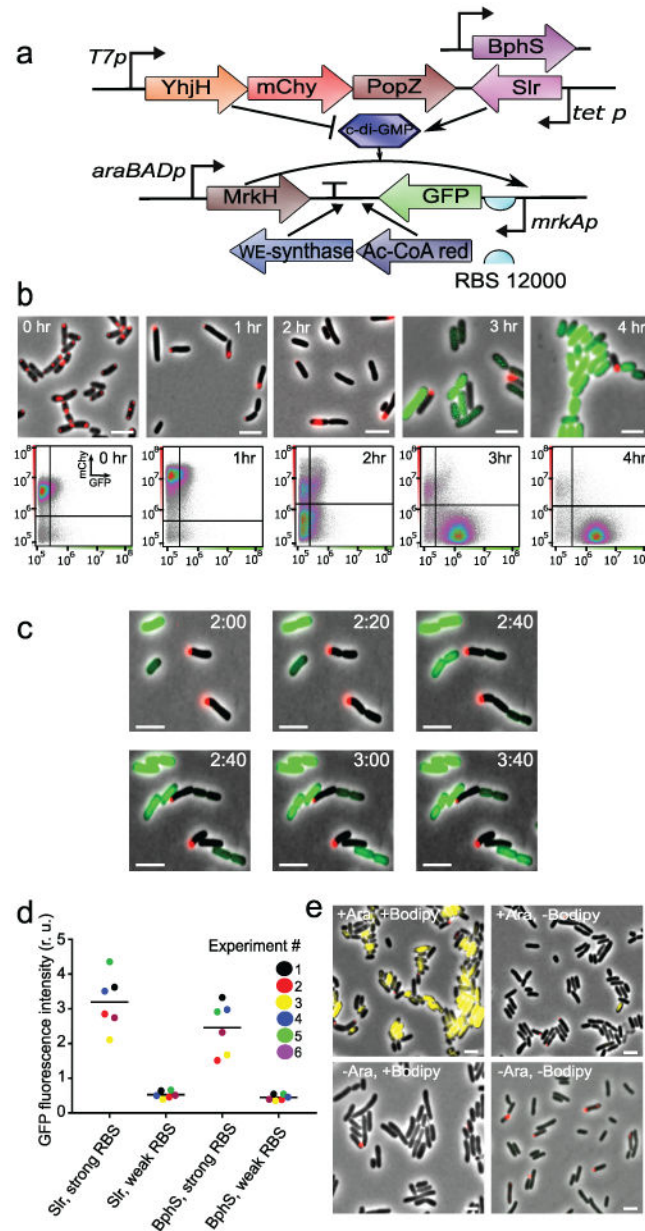
1. Paul K, Nieto V, Carlquist WC, Blair DF & Harshey RM The c-di-GMP Binding Protein YcgR Controls Flagellar Motor Direction and Speed to Affect Chemotaxis by a 'Backstop Brake' Mechanism. *Mol. Cell* 38, 128–139 (2010). [PubMed: 20346719]
2. Girgis HS, Liu Y, Ryu WS & Tavazoie S A comprehensive genetic characterization of bacterial motility. *PLoS Genet.* 3, 1644–1660 (2007). [PubMed: 17941710]
3. Datsenko K. a & Wanner BL One-step inactivation of chromosomal genes in *Escherichia coli* K-12 using PCR products. *Proc. Natl. Acad. Sci. U. S. A* 97, 6640–5 (2000). [PubMed: 10829079]
4. Ryu M & Gomelsky M Near-infrared Light Responsive Synthetic c – di-GMP Module for Optogenetic Applications. *ACS Synth. Biol.*, 11, 802–810 (2013).
5. Chin KH et al. Structural polymorphism of c-di-GMP bound to an EAL domain and in complex with a type II PilZ-domain protein. *Acta Crystallogr. Sect. D Biol. Crystallogr* 68, 1380–1392 (2012). [PubMed: 22993092]
6. Ong NTX & Tabor JJ A miniaturized *E. coli* green light sensor with high dynamic range. *ChemBioChem*, 19, 1255–1258 (2018). [PubMed: 29420866]

**Figure 1:**

A method for using polar asymmetry to generate two distinct cell types. (a) PopZ, which forms a macromolecular structure that becomes localized to *E. coli* cell poles, is part of a tripartite fusion protein that includes a phosphodiesterase (PDE) and a mChy tag. A diguanylate cyclase (DGC) is expressed at low levels and distributed throughout the cytoplasm. After transient expression of the PopZ fusion protein, the next cell division is asymmetric with respect to the inheritance of PopZ and the accumulation of c-di-GMP levels via PDE and DGC activities. (b) A genetic circuit for generating asymmetric cell division with respect to c-di-GMP signaling. (c) Observation of polar asymmetry and asymmetric cell division. In cells bearing plasmid pBad-YmP, YhjH-mChy-PopZ expression was induced with arabinose for two hours, washed to remove the inducer, then mounted on an agarose pad for observation of growth and division by time-lapse fluorescent microscopy. Three independent trials produced similar results. Scale bars 2 $\mu$ m.



**Figure 2:** Direct visualization of c-di-GMP levels in asymmetrically dividing cells using a split-GFP reporter. (a) Components for controlling c-di-GMP levels on plasmid pBad-YmP-BphS or pBad-YmP-Slr (top), and components for detecting c-di-GMP on plasmid pMQ132-splitGFP (bottom). (b) Asymmetric cell division after transient expression of YhjH-mChy-PopZ. Split-GFP is assembled in cells with high c-di-GMP (green signal). (c) Observation of split-GFP reporter in asymmetrically dividing cells, with Slr (plasmid pBad-YmP-S) as DGC. Aliquots of cells were analyzed by fluorescence microscopy (upper panel, five independent trials produced similar results) and flow cytometry (bottom panel, from a single trial) over a 4 hour time course of growth in liquid media following a pulse of YhjH-mChy-PopZ expression. For flow cytometry data, fluorescence intensity in GFP and mChy channels is plotted on the X and Y axis, respectively. Scale bars 2 $\mu$ m.

**Figure 3:**

Differential gene expression in asymmetrically dividing cells. (a) Components for controlling *c*-di-GMP levels on plasmid pAC-YmP-B or pAC-YmP-S (top), and components for *c*-di-GMP dependent expression of GFP on plasmid pB-Mrk-GFP or pB-Mrk-rbs-GFP (bottom). pB-Mrk-rbsGFP was further modified by inserting biosynthetic enzymes in the reporter element (plasmid pBad-M-G-W). (b) Aliquots of cells bearing plasmids pAC-YmP-S and pB-Mrk-rbsGFP were analyzed by fluorescence microscopy (upper panel, five independent trials produced similar results) and flow cytometry (bottom panel, six independent trials produced similar results) over a four hour time course in liquid media following a 1.5 hour pulse of YhjH-mChy-PopZ expression. (c) A time-lapse image series of cells from b, starting at the 2 hour point of the time course. Three independent trials

produced similar results. (d) Average GFP intensity of Yjh-mChy-PopZ negative cells at the four hour time point in strains bearing different circuit components (bar). Like colors show results from six independent trials. (e) Cells bearing plasmids pAC-YmP-S and pBad-M-G-W, 4 hours after the end of a pulse of Yjh-mChy-PopZ expression (red signal), with MrkH induction and Bodipy staining (yellow signal) as variables. The Bodipy signal is significantly brighter than GFP, which is not visible. Three independent trials produced similar results. Scale bars 2 $\mu$ m.

Author Manuscript

Author Manuscript

Author Manuscript

Author Manuscript

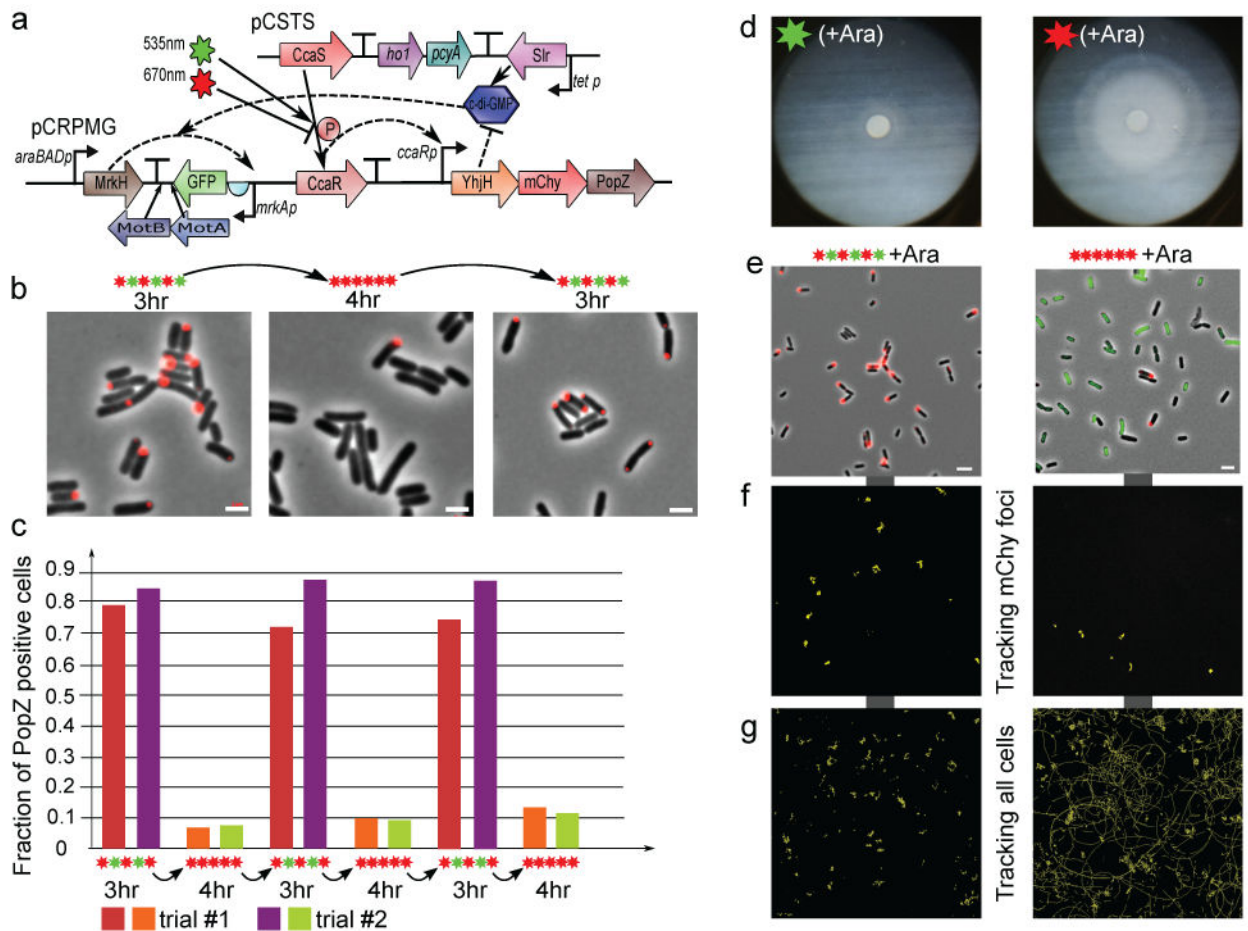


**Figure 4.** Control of asymmetric cell division by light. (a) pCSTS encodes a light-regulated histidine kinase, CcaS, genes for chromophore synthesis (*ho1*, *pcyA*), and Slr under the leaky *Tet-p* promoter. pCRPMG encodes the CcaR response regulator, YhjH-mChy-PopZ under control of the *ccaRp* promoter, MrkH under control of *araBADp*, and the GFP reporter element under *mrkAp*. (b-c) Changes in the percentage of YhjH-mChy-PopZ positive cells over multiple cycles of light stimulation in liquid culture. Microscope images were collected (b) and quantified (c) at the end of the indicated period of light exposure. Bar heights indicate the fraction of YhjH-mChy-PopZ positive cells in the culture during two independent trials. 400-1000 cells were counted for each sample at each time point. (d-h) Effects of light exposure on cell motility. *motA-motB* cells were transformed with pCSTS and pCRPMG + *motA-motB* plasmids. Five independent trials produced similar results. (d) shows cell motility in soft agar plates exposed to green or red light. (e) shows fluorescence images of cells from the cultures used to assess motility. To assess motility, movies of cells in liquid suspension were acquired using mChy fluorescence or phase contrast microscopy, and tracking software (f,g) was used to trace the movements of cells over 15 seconds (yellow lines). Scale bars 2 $\mu$ m.